Author Manuscript

Author Manuscript

Author Manuscript

Author Manuscript

HHS Public Access

Author manuscript

Antiviral Res. Author manuscript; available in PMC 2018 August 01.

Published in final edited form as:

Antiviral Res. 2017 August ; 144: 164–172. doi:10.1016/j.antiviral.2017.06.014.

Efficacy and Cytotoxicity in Cell Culture of Novel α-Hydroxytropolone Inhibitors of Hepatitis B Virus Ribonuclease H

Elena Lomonosova[1,2], **Jil Daw**[1], **Aswin K. Garimallaprabhakaran**[3], **Nana B. Agyemang**[3], **Yashkumar Ashani**[3], **Ryan P. Murelli**[3,4], and **John E. Tavis**[1,2,*]

[1]Department of Molecular Microbiology and Immunology, Saint Louis University School of Medicine, Saint Louis, MO USA

[2]Saint Louis University Liver Center, Saint Louis, MO USA

[3]Department of Chemistry, Brooklyn College, City University of New York, Brooklyn, NY USA

[4]PhD Program in Chemistry, The Graduate Center of The City University of New York, New York, NY USA

Abstract

Chronic Hepatitis B virus (HBV) infection is a major worldwide public health problem. Current direct-acting anti-HBV drugs target the HBV DNA polymerase activity, but the equally essential viral ribonuclease H (RNaseH) activity is unexploited as a drug target. Previously, we reported that α–hydroxytropolone compounds can inhibit the HBV RNaseH and block viral replication. Subsequently, we found that our biochemical RNaseH assay underreports efficacy of the α-hydroxytropolones against HBV replication. Therefore, we conducted a structure-activity analysis of 59 troponoids against HBV replication in cell culture. These studies revealed that antiviral efficacy is diminished by larger substitutions on the tropolone ring, identified key components in the substitutions needed for high efficacy, and revealed that cytotoxicity correlates with increased lipophilicity of the α-hydroxytropolones. These data provide key guidance for further optimization of the α-hydroxytropolone scaffold as novel HBV RNaseH inhibitors.

Keywords

HBV; RNaseH; Tropolones; Antiviral; QSAR

1. Introduction

Chronic hepatitis B virus (HBV) infection is a major global public health problem affecting an estimated 240–350 million people and causing about 1 million annual deaths worldwide from cirrhosis, liver failure, and hepatocellular carcinoma (Lavanchy, 2005; Trepo et al.,

*Corresponding Author. 1100 S. Grand Blvd., Saint Louis, MO 63104 USA. tavisje@slu.edu. Phone 321-977-8893. Fax 314-977-8717.

Publisher's Disclaimer: This is a PDF file of an unedited manuscript that has been accepted for publication. As a service to our customers we are providing this early version of the manuscript. The manuscript will undergo copyediting, typesetting, and review of the resulting proof before it is published in its final citable form. Please note that during the production process errors may be discovered which could affect the content, and all legal disclaimers that apply to the journal pertain.

Author Manuscript Author Manuscript Author Manuscript Author Manuscript

2014). Two categories of drugs are used in anti-HBV therapy: the interferons, including standard interferon- α and pegylated interferon-α, and nucleos(t)ide inhibitors of HBV polymerase (Lok et al., 2016). Monotherapy with a nucleos(t)ide analogue is the standard of care for many patients. However, these therapies rarely cure the infection and the nucleos(t)ide analogs require life-long administration to limit disease in most patients. Therefore, better anti-viral drugs are urgently needed to further reduce disease progression, with the ultimate goal of curing the infection.

HBV has DNA genome that is replicated via reverse transcription. The multifunctional HBV polymerase protein catalyzes conversion of the viral pregenomic RNA into the mature viral partially double-stranded relaxed circular DNA. This complex process includes DNA synthesis on both RNA and DNA templates, three nucleic acid strand transfers, and hydrolytic cleavage of the RNA in the RNA/DNA heteroduplex that is a key intermediate during reverse transcription. Both the reverse transcriptase (RT) and ribonuclease H (RNaseH) activities of the HBV polymerase protein are essential for HBV replication. However, all currently approved direct-acting anti-HBV drugs are RT inhibitors, whereas RNaseH inhibitors are yet to be developed. Recently we identified several classes of compounds that effectively inhibit both HBV RNaseH activity and viral replication (Cai et al., 2014; Edwards et al., 2017; Hu et al., 2013; Lu et al., 2015; Tavis et al., 2013). Many of the best inhibitors are α-hydroxytropolones (Lu et al., 2015).

The troponoids (tropones, tropolones, α-hydroxytropolones, and their derivatives) are aromatic compounds that differ from benzenoids both electronically due to their tropylium character and geometrically due to their unique seven-membered ring structure (Fig. 1) (Liu et al., 2014). To date, about 200 naturally occurring tropolones have been identified (Bentley, 2008; Zhao, 2007). Most troponoids were isolated from plants and fungi, but methods have been developed to synthesize them (reviewed in (Liu et al., 2014)), including the α-hydroxytropolones (reviewed in (Meck et al., 2014)). Troponoids have powerful antibacterial and antifungal activities (Baillie et al., 1950; Zhao, 2007). In addition, many other biological effects such as antiviral (Boguszewska-Chachulska et al., 2006; Budihas et al., 2005; Miyamoto et al., 1998b), antitumor and antiproliferative (Li et al., 2016; Miyamoto et al., 1998a; Oblak et al., 2012), and anti-inflammatory (Rekka et al., 2002) activities are associated with troponoids. Thus, troponoids hold promise to be developed into new medicines for a range of diseases.

The tropolones and α-hydroxytropolones (Fig. 1) have two or three contiguous hydroxyl/carbonyl groups, respectively, oriented to efficiently coordinate divalent cations within metalloenzymes (Bryant and Fernelius, 1954; Day and Cohen, 2013). Therefore, tropolones can inhibit metalloenzymes (Fullagar et al., 2013; Hirsch et al., 2014; Ismaya et al., 2011; Kim and Uyama, 2005), with the tropolones being able to inhibit enzymes with a single divalent cation and the α-hydroxytropolones being able to inhibit enzymes with two divalent cations. Recently we found that the α-hydroxytropolones can suppress HBV replication by inhibiting the HBV RNaseH activity (Hu et al., 2013; Lu et al., 2015; Tavis et al., 2013). Thirteen of 51 α-hydroxytropolones inhibited the HBV RNaseH enzyme *in vitro*, with the best 50% inhibitory concentration (IC_{50}) being 2.3 μM. Six of ten compounds tested in cell culture suppressed HBV replication, with the best 50% effective concentration (EC_{50}) being

Author Manuscript Author Manuscript Author Manuscript Author Manuscript

0.34 μM. Moderate cytotoxicity was observed for all compounds, with 50% cytotoxic concentrations (CC_{50}) ranging from 25 to 79 μM (Lu et al., 2015).

We hypothesized that selectivity and potency of the α-hydroxytropolones could be improved against HBV through medicinal chemistry optimization. Here, we report our recent advances in this hit-to-lead drug development effort that includes evaluation of 46 α-hydroxytropolones and 13 additional troponoids against HBV replication in culture.

2. Materials and Methods

2.1. Compounds

Compounds used in this study were acquired commercially or were synthesized as described below. Compounds #61–63 were purchased from ChemBridge (San Diego, CA), and compounds #46–57 and 195 were acquired from the NCI Developmental Therapeutics Program. Compound #172 was synthesized according to the procedure of Takeshita et al. (Takeshita et al., 1986). Compounds #106–120, 143–147, 273–274, and 335 were synthetized from kojic acid as previously described (D'Erasmo et al., 2016; Hirsch et al., 2014; Ireland et al., 2016; Meck et al., 2012; Williams et al., 2013). Compounds #280, 308–313, 315, and 317–319 were synthesized as described (Donlin et al., 2017). Compounds #261–264 were made using the Banwell method (Banwell et al., 1991). Compounds were ≥ 95% pure by ^{1}H NMR analysis. Synthesis and characterization of #257–259, 334, 336 and 347 can be found in the supporting information. All compounds were dissolved in DMSO (Sigma, St. Louis, MO) at 10 mM and stored at −80° C.

2.2. Cell culture

HepDES19 is a stably transformed HepG2-derived cell line carrying a tetracycline-repressible HBV genomic construct that supports HBV replication upon withdrawal of tetracycline (Guo et al., 2007). HepDES19 cells were maintained at 37°C with 5% CO_2 in DMEM/F12 medium (Fisher, Hampton, NH) supplemented with 100 U of penicillin/mL, 10 μg of streptomycin/mL, and 10% fetal bovine serum (Fisher, Hampton, NH) in the presence of 1 μg/mL of tetracycline. HEK293 is a human embryonic kidney cell line. LX-2 is human hepatic stellate cell line (Xu et al., 2005). HEK293 and LX2 were grown at 37°C with 5% CO_2 in DMEM (Fisher, Hampton, NH) supplemented with 100 U of penicillin/mL, 10 μg of streptomycin/mL, and 10% fetal bovine serum (Fisher, Hampton, NH).

2.3. EC_{50} determination

EC_{50} values for the compounds were determined by plating HepDES19 cells at 0.3×10^6 cells/well in 12-well plates in medium without tetracycline to induce HBV DNA replication. 48 hours later cells were treated with medium containing antiviral compounds or DMSO as a vehicle control without tetracycline. Encapsidated HBV DNA was then extracted, and quantitative PCR (qPCR) was performed with a strand-preferential assay with TaqMan reagents as described (Lomonosova and Tavis, 2017). The amounts of plus- and minus-polarity DNA strands were calculated as the percentage relative to the quantity of DNA in DMSO-treated cells. EC_{50} values were calculated from the decline in plus-polarity DNA

Author Manuscript Author Manuscript Author Manuscript Author Manuscript

levels with GraphPad Prism software using the nonlinear regression log(inhibitor) vs. response algorithm.

2.4. Cytotoxicity

Cytotoxicity was assessed by MTS assay. HepDES19, HEK293 or LX-2 cells were seeded into 96-well plates at a density of 2×10^4 cells/well and exposed to compounds with a treatment schedule identical to that used for the HBV replication inhibition assays. Following compound treatment, 20 μL [3-(4,5-dimethylthiazol-2-yl)-5-(3-carboxymethoxyphenyl)-2-(4-sulfophenyl)-2H–tetrazolium, inner salt] (MTS) (Promega, Madison, WI) solution containing the electron coupling reagent phenazine methosulfate (PMS) (Promega, Madison, WI) was added to the cells to a final concentration of MTS 0.33 mg/mL. Cells were incubated at 37°C for 1 hour, and absorbance was measured at 490 nm. Cytotoxicity was calculated as the percentage relative to cytotoxicity determined in DMSO-treated cells. CC_{50} values were calculated with GraphPad Prism software using the nonlinear regression log(inhibitor) vs. response algorithm.

2.5. Calculation of physicochemical parameters

ChemAxon software was used to calculate six parameters for the active compounds: octanol-water partitioning coefficient (logP), octanol-water distribution coefficient at pH = 7.4 ($logD_{7.4}$), polar surface area at pH = 7.4 (PSA) (Ertl et al., 2000), molecular polarizabilty (MP) at pH = 7.4 (Hansch et al., 2003), Van der Waals surface area (VdWSA) at pH = 7.4 (Ferrara et al., 2002), and molecular refractivity (MR) (Ghose et al., 1999; Viswanadhan et al., 1989). Solubility forecast index (SFI) was calculated by summing $logD_{7.4}$ and the number of aromatic rings ($SFI = logD_{7.4} + \#Ar$) (Hill and Young, 2010).

2.6. Regression analysis

Linear regression analyses were performed with RStudio using an R script. The regression coefficients were initially estimated for the complete set of physicochemical parameters that yielded p-values less than 0.01. Next, the least-significant predictor was eliminated from the model and the data were refit. This was repeated until all remaining regression coefficients were significant at confidence levels ≤ 0.01%.

3. Results and Discussion

We previously identified the α-hydroxytropolone natural product β-thujaplicinol as a potent inhibitor of HBV RNaseH that suppresses HBV replication in cell culture with EC_{50} = 1 μM (Hu et al., 2013; Tavis et al., 2013). Subsequent studies on a library of fully synthetic α-hydroxytropolones led to identification of several other HBV RNaseH inhibitors that could block viral replication (Lu et al., 2015). Importantly, one of these molecules was #110, which has an EC_{50} of 0.34 μM in cell-based antiviral assays. Paradoxically, most of these α–hydroxytropolones were less effective in enzymatic RNaseH inhibition assays than they were against viral replication. This quantitative discord between the IC_{50}s and EC_{50}s appears to primarily be due to limitations in our ability to measure RNaseH activity, not failure of the compounds to act against the RNaseH. This is because the RNaseH inhibitors yield an RNaseH-deficient phenotype in cells (i.e., truncated minus polarity DNAs,

Author Manuscript Author Manuscript Author Manuscript Author Manuscript

accumulation of RNA:DNA heteroduplexes, and lack of plus-polarity DNA), not just an overall reduction in DNA accumulation (Hu et al., 2013). Also, the bacterially expressed and purified recombinant RNaseH domain used for the enzymatic RNaseH inhibition assays can be inhibited by the compounds we identified, but the recombinant enzyme is only a part of the full HBV polymerase protein, and may not completely recapitulate the behavior of the full length protein. Thus, while the enzymatic inhibition assay was key to identifying the α-hydroxytropolones as a promising pharmacophore for HBV RNaseH inhibitor development, limitations to the sensitivity of the biochemical assay indicate that evaluation of cell-based antiviral activity is necessary to provide meaningful a structure-activity relationship to guide medicinal chemistry improvement. Our prior studies gained cell-based antiviral EC_{50} values for just two natural product and four synthetic α-hydroxytropolones (Lu et al., 2015). Here, we detail cell-based antiviral activity of 46 α-hydroxytropolones and an additional 13 troponoids with the goal of identifying promising medicinal chemistry avenues to optimize efficacy and minimize cytotoxicity.

3.1. Efficiency of troponoids against HBV replication and cytotoxicity

This sublibrary of troponoids was screened against HBV using a cell culture replication inhibition assay that measures suppression of the HBV plus-polarity DNA strand because synthesis of the plus-polarity DNA strand cannot proceed if the RNaseH activity is blocked, whereas the minus-polarity DNA strand is relatively unaffected by RNaseH inhibitors. All but eight of the 46 α-hydroxytropolones suppressed HBV replication (Table 1), whereas all 13 of the other troponoids were inactive (Suppl. Table 1). All tested tropolones that suppress HBV plus-strand DNA have either no effect on minus-strand DNA synthesis or inhibited it at significantly higher concentrations than plus-strand (Suppl. Table 2). Thirty-six of the 38 active α-hydroxytropolones had EC_{50} values <10 μM and eight had EC_{50} values of <1 μM (Table 1). The most effective of the new compounds tested were #107, 280, 336 and 347, which had EC_{50} values of 0.4 ± 0.2, 0.5 ± 0.1, 0.4 ± 0.2, and 0.6 ± 0.4 μM, respectively.

Cytotoxicity of the troponoids in this sublibrary was determined in HepDES19 cells using an MTS assay in parallel with the replication inhibition activity measures to establish the specificity of anti-viral effects. CC_{50} values for the 38 compounds active against HBV replication ranged from 17 to >100 μM, with 19 of these active compounds having CC_{50} values >50 μM (Table 1).

3.2. Therapeutic indexes and drug-like properties of the troponoids

Therapeutic index (TI) values for each compound were calculated based on the MTS cytotoxicity assay as TI = CC_{50}/EC_{50} and ranged from 3 to >200 (Table 1). We selected the 11 compounds with highest TI values and further investigated their potential cytotoxicity in HEK293 kidney cells and LX-2 hepatic stellate cells (Table 2). All compounds had CC_{50}s in HEK293 and LX-2 cells by the MTS assay that were the same or higher than in HepDES19 cells, indicating a lack of cell-type specific cytotoxicity.

We next evaluated these 11 best α-hydroxytropolones for compliance with Lipinski's Rule of Five (Lipinski et al., 1997) as a measure of their drug-like properties. The rule states that a compound is more likely to exhibit poor absorption or permeation when two or more of the

Author Manuscript Author Manuscript Author Manuscript Author Manuscript

following physicochemical criteria are fulfilled: the molecular weight is greater than 500, the calculated logP is greater than five, there are more than five hydrogen-bond donors, and the number of hydrogen-bond acceptors is greater than ten. All selected α-hydroxytropolones passed the Rule of Five with zero violations (Suppl. Table 3).

3.3. Structure-activity relationships against HBV replication in culture

3.3.1. Mono-substituted α-hydroxytropolones—The first α–hydroxytropolone identified as an HBV RNaseH inhibitor was compound #46, which has a single isopropyl group on the troponoid ring (Hu et al., 2013; Tavis et al., 2013). To gauge the importance of this appendage, we tested compound #210, where the isopropyl group was truncated to a methyl group, and the parent α-hydroxytropolone #172, where the group was removed completely. The three molecules had equivalent antiviral potency, with EC_{50} values of 1.0, 1.2, and 1.7 μM ($p = 0.71$, ANOVA: single factor) (Table 1). Inclusion of larger 3- and 4-biphenyl groups on the tropolone ring (compounds #263 and 264) caused slight but statistically insignificant loss of anti-HBV efficiency (EC_{50} 2.4 ± 0.7 and 2.8 ± 0.7, $p = 0.54$ and 0.38, respectively, student's t-test) over #172. This suggests that bulky aromatic substituents in the R^2 position are tolerated but trended to lesser potency. In contrast, the R^2 bromide-containing compound #261 was six-fold less potent than #172 and 11-fold less potent than #46. This decreased potency could be due to the bromine directly impacting efficacy or from it destabilizing the molecule in tissue culture. Overall, substituents in R^2 position on the tropolone ring could be arranged as H ≡ short aliphatic < aromatic << bromine in order of decreasing efficiency against HBV replication.

3.3.2. Di-substituted α-hydroxytropolones where R^1 = Me and R^2 = aromatic—The majority of the synthetic α-hydroxytropolones were generated through an oxidopyrylium cycloaddition/ring-opening strategy developed in the Murelli lab (Meck et al., 2012), and thus mostly contain a methyl group at R^1 as a synthetic handle plus either an aromatic or carbonyl-containing appendage at R^2.

Among the aromatic-containing molecules, we previously identified compounds #112 and 113 as inhibitors of HBV replication with EC_{50} values of 2.5 ± 1.3 and 4.2 ± 0.8 μM (Table 1) (Lu et al., 2015). These compounds and three compounds in the current sublibrary (#114, 119, and 146) have similar structural properties (methyl group in R^1 position and aryl group in R^2 position) and have similar EC_{50} values in the low micromolar range. The best molecules from the series were the nitrophenyl-containing #112 and 1-napthyl-containing #146, which were still two- to three-fold less potent than #210. Furthermore, four additional aromatic-containing α-hydroxytropolones (#115, 144, 145, and 147, Suppl. Table 1) did not inhibit HBV replication. Therefore, this series was not pursued further.

3.3.3. Di-substituted α-hydroxytropolones where R^1 = Me and R^2 = carbonyl-containing appendages plus the sulfonyl-containing compound #336—Our structure-function analysis did suggest benefits of having a carbonyl at R^2. Highlighting this is the methyl ketone-containing compound #110, which was previously identified as the most potent troponoid with EC_{50} = 0.3 ± 0.03 μM (Lu et al., 2015), three- to four-fold more potent than #210 (Table 1), which differs only by the absence of a methyl ketone at R^2.

Author Manuscript Author Manuscript Author Manuscript Author Manuscript

However, similar aliphatic ketone-containing α-hydroxytropolones (#120, 143, 173, and 310) were all significantly less potent, demonstrating that there is little room for growth at this position.

This conclusion is emphasized by two other carbonyl-containing α-hydroxytropolones, the methyl ester-containing compound #274 and ethyl ester-containing #109. While #274 has activity on par with #172 (EC_{50} = 1.1 μM), the subtle change from a methyl ester to an ethyl ester in #109 dropped potency four-fold (EC_{50} = 4.3 μM) compared to #210 (Table 1). On the other hand, changing to a carboxylic acid appendage (#319), while representing an even smaller group, was about four-fold less potent than #172. In this case, it is possible the anionic nature of the presumed carboxylate form could limit passive diffusion across biological membrane (Ballatore et al., 2013), and this could explain both its lower potency and cytotoxicity.

Aromatic ketone-containing molecules were somewhat more effective than #172. Several α-hydroxytropolones with smaller aromatic ketone-containing appendages (#111, 308, 309, 311, 312, and 313) had potency comparable to #172, although they were all two- to fivefold less potent than #110 (Table 1). Still larger aromatic ketones, such as compounds with napthyl (#315) and biaryl (#118, 257, 258 and 259) appendages, were two- to six-fold less potent than #172, or six- to 29-fold less potent than #110, and three additional larger biaryl ketones had no antiviral activity (#255, 256, and 260, Suppl. Table 1).

Taken together, these data suggest that carbonyl appendages at R^2 can be beneficial for enhanced efficacy, but the appendages must remain small. One possible explanation for these enhanced properties could be electronic, as the presence of the ketone could either enhance the tropylium characteristic of the tropolone and/or impact the acidity of the tropolone hydroxyls. It is also plausible that the carbonyl could participate in a hydrogen-bonding interaction when bound to the enzyme. Either way, we were curious about the potential impact on efficacy attendant with a change from a carbonyl to a sulfone, as this would have both greater electron-withdrawing properties and introduce two Lewis basic oxygens that could participate in hydrogen-bonding. We thus synthesized and tested the α-hydroxytropolone #336, a sulfonyl analog of the phenyl ketone #111. Compound #336 was twice as potent as #111, and had comparable, if not lower, cytotoxicity (Table 1). A greater survey of sulfonyl-containing α-hydroxytropolones is underway.

3.3.4. Tri-substituted α-hydroxytropolones and identification of potent lactones #280 and 347—While one carbonyl moiety on the tropolone appears to be beneficial, the two-fold decrease in activity of #106 compared to #274 (Table 1) suggests that addition of a second carbonyl at R^3 may be deleterious. So too was the impact of an additional bromide (#334 and 335), which decreased replication inhibition by almost an order of magnitude compared to their non-brominated counterparts (#110 and 274). It is unclear if this loss in potency was due to a direct impact of the bromide or whether the bromide-containing compounds were unstable in cells. Efforts are underway towards synthesis and testing of alternative halogen-containing α-hydroxytropolones to determine if this is a general phenomenon of halogens or is specific to the bromide derivatives.

Author Manuscript Author Manuscript Author Manuscript Author Manuscript

One of the more dramatic structure-function relationships was observed when comparing three molecules with methyl esters at both R^2 and R^3 that varied at R^1. We had previously observed that compound #106 (with a methyl group at R^1) was typical with respect to potency among the synthetic α-hydroxytropolones, with an EC_{30} of 2.7 μM (Lu et al., 2015). However, potency dropped about five-fold (EC_{50} = 15 μM) when this methyl group was instead a methoxymethylene (#108) (Table 1). A similar decrease in activity from #106 to 108 was also observed against the HIV RNaseH, where enzymatic IC_{50} values were 0.23 and 1.0 μM, respectively (Murelli et al., 2016). On the other hand, when R^1 was instead a chloromethylene (#107), a dramatic increase in anti-HBV activity was observed, with an EC_{50} value of 0.4 μM, which is six-fold more potent than #106. This is not only in stark contrast to the behavior of #107 against the HIV RNaseH (IC_{50} = 0.8 μM), where it is closer in activity to #108 than to #106, but is also in contrast to HBV RNaseH enzymatic assays, where it is also less potent than #106 (Lu et al., 2015). Given the high metabolic activity expected in hepatocyte-derived cells, we questioned the stability of #107, suspecting that it might lactonize in the course of the assays to generate compound #280 (Fig. 2). Lactonization of #107 to 280 was reported by our labs previously, and was found to take place under fairly mild conditions (0.05% trifluoroacetic acid in water/acetonitrile) (Donlin et al., 2017). Here, we suggest that this lactonization (between #107 to 280) may take place in cell cultures. Indeed, activity of the lactone compound #280 was virtually equivalent to #107, supporting this hypothesis. Therefore, an additional lactone, #347, was synthesized. It also demonstrated comparable activity against HBV replication as #107. *In vivo* lactonization has previously been suggested to occur for some of the cholesterol-lowering drugs, statins, either through intestinal non-enzymatic reactions due to the low pH, or by an intracellular enzymatic mechanism mediated by uridine diphosphate (UDP)-glucuronosyltransferases (Kearney et al., 1993; Prueksaritanont et al., 2002). It is unknown if the same mechanisms are involved in possible lactonization of compound #107. Excitingly, while the antiviral efficacy of several molecules in this study (#107, 280, 336, and 347) approached that of #110, their cytotoxicity was significantly reduced compared to #110, providing an enhanced therapeutic index (up to 2-fold for compound #107). Our current hypotheses to explain the higher activity of the lactone is that rotational restriction of the lactone could limit entropic penalties to binding and/or provide greater overlap between the carbonyl and the tropolone, enhancing tropylium characteristics that could be beneficial to inhibition.

3.4. Structure-cytotoxicity relationships

We conducted a structure-cytotoxicity analysis to determine if there were any prominent components of the compounds that promoted cytotoxicity. First, we analyzed the effect of the α-hydroxyl group by comparing the CC_{50} values of 45 α–hydroxytropolones and 13 tropolones without the α–hydroxyl group. Logistic regression revealed that the average CC_{50} for troponoids with α-hydroxy group was significantly lower than for troponoids without α-hydroxy group (56 μM vs 79 μM, $p = 0.017$). This effect correlated with a hydroxyl at the α position on the ring because changing this hydroxyl group to a methoxy group (compounds #273 and 318) or bromine group (compound #54) resulted in less toxic compounds with CC_{50} values >90 μM (Suppl. Table 1). We also analyzed the contribution of substitution type on cytotoxicity. In general, compounds with aromatic groups in the R^2

Author Manuscript Author Manuscript Author Manuscript Author Manuscript

position were more toxic than compounds with smaller aliphatic substitutions. Furthermore, several of the more toxic compounds (CC_{50} < 35 μM) shared a common biaryl component at R^2 (compounds #118, 115, 255, 257, 258, 259, and 264). It is not surprising that tropolones containing biaryls are the most toxic. It was demonstrated previously that biphenyl moieties could bind to a wide range of proteins (Hajduk et al., 2000) and other molecules through a variety of interactions with aromatic and hydrophobic residues (McGaughey et al., 1998), polar amides (van der Spoel et al., 1996) or hydroxyl (Sapse et al., 1992) groups, and even positively charged moieties (Mecozzi et al., 1996).

3.5. Quantitative structure-activity relationships (QSAR)

Physicochemical properties of the compounds can both influence their toxicological profile (Blagg, 2006; Raies and Bajic, 2016). Many of these chemical parameters can be calculated from the compounds' structures, so we determined if there were quantitative correlations between calculated physicochemical properties of tropolones and anti-HBV efficacy and cytotoxicity. Seven molecular descriptors were used: octanol-water partitioning coefficient (logP), octanol-water distribution coefficient at pH = 7.4 ($logD_{7.4}$), solubility forecast index (SFI) as calculated by summing $logD_{7.4}$ and the number of aromatic rings (Hill and Young, 2010), polar surface area at pH = 7.4 (PSA) (Ertl et al., 2000), molecular polarizabilty at pH = 7.4 (MP) (Hansch et al., 2003), Van der Waals surface area at pH = 7.4 (VdWSA) (Ferrara et al., 2002), and molecular refractivity (MR) (Ghose et al., 1999). Suppl. Table 4 contains these predicted physicochemical values for a key set of tropolones. Linear regression was performed for these parameters to identify correlations with the anti-HBV efficiency and cytotoxicity. No correlations were found between efficiency and physicochemical properties of the tropolones. However, strong correlations were observed between physicochemical properties and cytotoxicity of tropolones.

Lipophilicity is an especially important drug-like property, measured by logP and logD (Leeson and Springthorpe, 2007; Linnankoski et al., 2006; van De Waterbeemd et al., 2001), that can influence drug toxicity (Cronin, 2006) as well as other phenotypic features (van De Waterbeemd et al., 2001). We found a significant correlation of logP with cytotoxicity of α-hydroxytropolones (Suppl. Table 5, Fig. 3A). Tropolones with higher logP values are more cytotoxic than tropolones with lower logP. Similarly, $logD_{7.4}$ is also negative predictor of tropolones cytotoxicity (Suppl. Table 5). Lipophilicity can reflect a key event of molecular desolvation in transfer from aqueous phases to cell membranes and to proteins binding sites (Leeson and Springthorpe, 2007). If lipophilicity is too high, there is an increased likelihood of binding to multiple targets and enhancing cytotoxicity, and this may have contributed to cytotoxicity in our assays.

Recently, SFI was found to be a simple and effective predictor of solubility (Hill and Young, 2010). Its value is influenced by the number of aromatic rings in a molecule in addition to lipophilicity (measured by logD), as it was shown that increased aromaticity has negative impact on solubility (Ritchie and Macdonald, 2009). In our modeling, SFI as a single factor gave the strongest correlation of the α–hydroxytropolones' physicochemical descriptors with cytotoxicity (Suppl. Table 5, Fig. 3B). It was also suggested that keeping SFI <5 in compound design should improve probability of securing good physical properties (Hill and

Author Manuscript Author Manuscript Author Manuscript Author Manuscript

Young, 2010). Interestingly, separation of α–hydroxytropolones by SFI values (SFI = 1–5 vs. SFI > 5) also resulted in two subgroups of compounds with statistically different mean EC_{50}s (2.7 vs. 5.2, p = 0.02) (Fig. 4), implying that α-hydroxytropolones with SFI values from 1 to 5 might have higher anti-HBV efficiency in addition to better cytotoxicity profiles.

Recent studies have highlighted the importance of molecular polar surface area (PSA; the surface belonging to polar O and N atoms (Ertl et al., 2000)), on drug absorption (Hou et al., 2007; Linnankoski et al., 2006). Our analysis showed no significant correlation between PSA values and cytotoxicity for the α–hydroxytropolones (Suppl. Table 5). In contrast, modelling of Van der Waals surface area as well as molecular refractivity both resulted in significant correlations with cytotoxicity. Therefore, in addition to bulk lipophilicity, specific three-dimensional structural features including Van der Waals forces, polarizability and refractivity correlated with cytotoxicity for the α-hydroxytropolones (Suppl. Table 5).

Having found a few physicochemical properties to be associated with cytotoxicity of α-hydroxytropolones and given that these properties were not independent of each other, we performed multivariate linear regression including all parameters that were significant in univariant analyses. In this multivariate model, the logP, logD, and SFI values were not predictive of cytotoxicity. The final model included molecular polarizability, Van der Waals surface area, and molecular refractivity and yielded a good correlation with the observed toxicity with an adjusted R^2 value of 0.52 and p-value of 4.6×10^{-6} (Suppl. Table 5, Fig. 3C). In this model, the predicted cytotoxicity of α–hydroxytropolones increased linearly with molecular refractivity and decreased linearly with molecular polarizability and Van der Waals surface area.

4. Summary

Recent progress in the development of *in vitro* and *in vivo* models of HBV infection (Allweiss and Dandri, 2016) have helped to identify new targets for the development of anti-viral drugs that act against previously unexploited viral or cellular targets (Block et al., 2015). We previously identified the α–hydroxytropolone scaffold as an inhibitor of the HBV RNaseH, a novel drug target, and demonstrated that inhibiting the viral RNaseH efficiently blocks HBV genomic replication. Here, we systematically evaluated substitutions at the R^1, R^2, and R^3 positions on the tropolone ring of α–hydroxytropolones for their effects on anti-HBV replication and cytotoxicity. These studies indicated that efficacy is diminished by larger substitutions on the tropolone ring, identified key components in the substitutions needed for high efficacy, implied that efficacy may be enhanced by sulfonyl or lactone appendages, and revealed that cytotoxicity correlates with increased lipophilicity. These data will facilitate design of new tropolones with better efficacy against the HBV RNaseH and reduced cellular toxicity, with the goal of developing the α-hydroxytropolones as a new class of drugs to be used in combination with other inhibitors to block disease progression and potentially cure chronic HBV infections.

Supplementary Material

Refer to Web version on PubMed Central for supplementary material.

Author Manuscript Author Manuscript Author Manuscript Author Manuscript

Acknowledgments

We thank Marvin Meyers for helpful discussions. We thank Professor Scott L. Friedman, MD, Icahn School of Medicine at Mount Sinai for the gift of LX-2 cells. This work was supported by grants R01 AI122669 to JET and SC1 GM111158 to RPM.

References

Allweiss L, Dandri M. Experimental in vitro and in vivo models for the study of human hepatitis B virus infection. Journal of hepatology. 2016; 64:S17–S31. [PubMed: 27084033]

Baillie AJ, Freeman GG, Cook JW, Somerville AR. Antibacterial and antifungal activity of benztropolone. Nature. 1950; 166:65. [PubMed: 15439122]

Ballatore C, Huryn DM, Smith AB 3rd. Carboxylic acid (bio)isosteres in drug design. ChemMedChem. 2013; 8:385–395. [PubMed: 23361977]

Banwell MG, Cameron JM, Collis MP, Crisp GT, Gable RW, Hamel E, Lambert JN, Mackay MF, Reum ME, Scoble JA. The Palladium-Mediated Cross Coupling of Bromotropolones with Organostannanes or Arylboronic Acids - Applications to the Synthesis of Natural-Products and Natural Product Analogs. Aust J Chem. 1991; 44:705–728.

Bentley R. A fresh look at natural tropolonoids. Natural product reports. 2008; 25:118–138. [PubMed: 18250899]

Blagg J. Structure-activity relationships for In vitro and In vivo toxicity. Annu Rep Med Chem. 2006; 41:353–368.

Block TM, Rawat S, Brosgart CL. Chronic hepatitis B: A wave of new therapies on the horizon. Antiviral research. 2015; 121:69–81. [PubMed: 26112647]

Boguszewska-Chachulska AM, Krawczyk M, Najda A, Kopanska K, Stankiewicz-Drogon A, Zagorski-Ostoja W, Bretner M. Searching for a new anti-HCV therapy: synthesis and properties of tropolone derivatives. Biochemical and biophysical research communications. 2006; 341:641–647. [PubMed: 16438939]

Bryant BE, Fernelius WC. Formation constants of metal complexes of tropolone and its derivates II. Some alkyltropolones. J Am Chem Soc. 1954; 76:1696–1697.

Budihas SR, Gorshkova I, Gaidamakov S, Wamiru A, Bona MK, Parniak MA, Crouch RJ, McMahon JB, Beutler JA, Le Grice SF. Selective inhibition of HIV-1 reverse transcriptase-associated ribonuclease H activity by hydroxylated tropolones. Nucleic acids research. 2005; 33:1249–1256. [PubMed: 15741178]

Cai CW, Lomonosova E, Moran EA, Cheng X, Patel KB, Bailly F, Cotelle P, Meyers MJ, Tavis JE. Hepatitis B virus replication is blocked by a 2-hydroxyisoquinoline-1,3(2H,4H)-dione (HID) inhibitor of the viral ribonuclease H activity. Antiviral research. 2014; 108:48–55. [PubMed: 24858512]

Cronin MTD. The Role of Hydrophobicity in Toxicity Prediction. Curr Comput-Aid Drug. 2006; 2:405–413.

D'Erasmo MP, Masaoka T, Wilson JA, Hunte EM Jr, Beutler JA, Le Grice SF, Murelli RP. Traceless Solid-Phase alpha-Hydroxytropolone Synthesis. MedChemComm. 2016; 7:1789–1792. [PubMed: 28090282]

Day JA, Cohen SM. Investigating the selectivity of metalloenzyme inhibitors. Journal of medicinal chemistry. 2013; 56:7997–8007. [PubMed: 24074025]

Donlin MJ, Zunica A, Lipnicky A, Garimallaprabhakaran AK, Berkowitz AJ, Grigoryan A, Meyers MJ, Tavis JE, Murelli RP. Troponoids can inhibit growth of the human fungal pathogen Cryptococcus neoformans. Antimicrobial agents and chemotherapy. 2017

Edwards TC, Lomonosova E, Patel JA, Li Q, Villa JA, Gupta AK, Morrison LA, Bailly F, Cotelle P, Giannakopoulou E, Zoidis G, Tavis JE. Inhibition of hepatitis B virus replication by N-hydroxyisoquinolinediones and related polyoxygenated heterocycles. Antiviral research. 2017

Ertl P, Rohde B, Selzer P. Fast calculation of molecular polar surface area as a sum of fragment-based contributions and its application to the prediction of drug transport properties. Journal of medicinal chemistry. 2000; 43:3714–3717. [PubMed: 11020286]

Author Manuscript Author Manuscript Author Manuscript Author Manuscript

Ferrara P, Apostolakis J, Caflisch A. Evaluation of a fast implicit solvent model for molecular dynamics simulations. Proteins. 2002; 46:24–33. [PubMed: 11746700]

Fullagar JL, Garner AL, Struss AK, Day JA, Martin DP, Yu J, Cai X, Janda KD, Cohen SM. Antagonism of a zinc metalloprotease using a unique metal-chelating scaffold: tropolones as inhibitors of P. aeruginosa elastase. Chem Commun (Camb). 2013; 49:3197–3199. [PubMed: 23482955]

Ghose AK, Viswanadhan VN, Wendoloski JJ. A knowledge-based approach in designing combinatorial or medicinal chemistry libraries for drug discovery. 1. A qualitative and quantitative characterization of known drug databases. Journal of combinatorial chemistry. 1999; 1:55–68. [PubMed: 10746014]

Guo H, Jiang D, Zhou T, Cuconati A, Block TM, Guo JT. Characterization of the intracellular deproteinized relaxed circular DNA of hepatitis B virus: an intermediate of covalently closed circular DNA formation. Journal of virology. 2007; 81:12472–12484. [PubMed: 17804499]

Hajduk PJ, Bures M, Praestgaard J, Fesik SW. Privileged molecules for protein binding identified from NMR-based screening. Journal of medicinal chemistry. 2000; 43:3443–3447. [PubMed: 10978192]

Hansch C, Steinmetz WE, Leo AJ, Mekapati SB, Kurup A, Hoekman D. On the role of polarizability in chemical-biological interactions. Journal of chemical information and computer sciences. 2003; 43:120–125. [PubMed: 12546544]

Hill AP, Young RJ. Getting physical in drug discovery: a contemporary perspective on solubility and hydrophobicity. Drug discovery today. 2010; 15:648–655. [PubMed: 20570751]

Hirsch DR, Cox G, D'Erasmo MP, Shakya T, Meck C, Mohd N, Wright GD, Murelli RP. Inhibition of the ANT(2")-Ia resistance enzyme and rescue of aminoglycoside antibiotic activity by synthetic alpha-hydroxytropolones. Bioorganic & medicinal chemistry letters. 2014; 24:4943–4947. [PubMed: 25283553]

Hou T, Wang J, Zhang W, Xu X. ADME evaluation in drug discovery. 7. Prediction of oral absorption by correlation and classification. Journal of chemical information and modeling. 2007; 47:208–218. [PubMed: 17238266]

Hu Y, Cheng X, Cao F, Huang A, Tavis JE. beta-Thujaplicinol inhibits hepatitis B virus replication by blocking the viral ribonuclease H activity. Antiviral research. 2013; 99:221–229. [PubMed: 23796982]

Ireland PJ, Tavis JE, D'Erasmo MP, Hirsch DR, Murelli RP, Cadiz MM, Patel BS, Gupta AK, Edwards TC, Korom M, Moran EA, Morrison LA. Synthetic alpha-Hydroxytropolones Inhibit Replication of Wild-Type and Acyclovir-Resistant Herpes Simplex Viruses. Antimicrobial agents and chemotherapy. 2016; 60:2140–2149. [PubMed: 26787704]

Ismaya WT, Rozeboom HJ, Weijn A, Mes JJ, Fusetti F, Wichers HJ, Dijkstra BW. Crystal structure of Agaricus bisporus mushroom tyrosinase: identity of the tetramer subunits and interaction with tropolone. Biochemistry. 2011; 50:5477–5486. [PubMed: 21598903]

Kearney AS, Crawford LF, Mehta SC, Radebaugh GW. The interconversion kinetics, equilibrium, and solubilities of the lactone and hydroxyacid forms of the HMG-CoA reductase inhibitor, CI-981. Pharmaceutical research. 1993; 10:1461–1465. [PubMed: 8272408]

Kim YJ, Uyama H. Tyrosinase inhibitors from natural and synthetic sources: structure, inhibition mechanism and perspective for the future. Cellular and molecular life sciences : CMLS. 2005; 62:1707–1723. [PubMed: 15968468]

Lavanchy D. Worldwide epidemiology of HBV infection, disease burden, and vaccine prevention. Journal of clinical virology : the official publication of the Pan American Society for Clinical Virology. 2005; 34(Suppl 1):S1–S3.

Leeson PD, Springthorpe B. The influence of drug-like concepts on decision-making in medicinal chemistry. Nature reviews. Drug discovery. 2007; 6:881–890. [PubMed: 17971784]

Li J, Falcone ER, Holstein SA, Anderson AC, Wright DL, Wiemer AJ. Novel alpha-substituted tropolones promote potent and selective caspase-dependent leukemia cell apoptosis. Pharmacological research. 2016; 113:438–448. [PubMed: 27663262]

Author Manuscript Author Manuscript Author Manuscript Author Manuscript

Linnankoski J, Makela JM, Ranta VP, Urtti A, Yliperttula M. Computational prediction of oral drug absorption based on absorption rate constants in humans. Journal of medicinal chemistry. 2006; 49:3674–3681. [PubMed: 16759110]

Lipinski CA, Lombardo F, Dominy BW, Feeney PJ. Experimental and computational approaches to estimate solubility and permeability in drug discovery and development settings. Advanced drug delivery reviews. 1997; 23:3–25.

Liu N, Song W, Schienebeck CM, Zhang M, Tang W. Synthesis of Naturally Occurring Tropones and Tropolones. Tetrahedron. 2014; 70:9281–9305. [PubMed: 25400298]

Lok AS, McMahon BJ, Brown RS Jr, Wong JB, Ahmed AT, Farah W, Almasri J, Alahdab F, Benkhadra K, Mouchli MA, Singh S, Mohamed EA, Abu Dabrh AM, Prokop LJ, Wang Z, Murad MH, Mohammed K. Antiviral therapy for chronic hepatitis B viral infection in adults: A systematic review and meta-analysis. Hepatology. 2016; 63:284–306. [PubMed: 26566246]

Lomonosova E, Tavis JE. In Vitro Enzymatic and Cell Culture-Based Assays for Measuring Activity of HBV RNaseH Inhibitors. Methods Mol Biol. 2017; 1540:179–192. [PubMed: 27975316]

Lu G, Lomonosova E, Cheng X, Moran EA, Meyers MJ, Le Grice SF, Thomas CJ, Jiang JK, Meck C, Hirsch DR, D'Erasmo MP, Suyabatmaz DM, Murelli RP, Tavis JE. Hydroxylated tropolones inhibit hepatitis B virus replication by blocking viral ribonuclease H activity. Antimicrobial agents and chemotherapy. 2015; 59:1070–1079. [PubMed: 25451058]

McGaughey GB, Gagne M, Rappe AK. pi-Stacking interactions. Alive and well in proteins. The Journal of biological chemistry. 1998; 273:15458–15463. [PubMed: 9624131]

Meck C, D'Erasmo MP, Hirsch DR, Murelli RP. The biology and synthesis of alpha-hydroxytropolones. MedChemComm. 2014; 5:842–852. [PubMed: 25089179]

Meck C, Mohd N, Murelli RP. An oxidopyrylium cyclization/ring-opening route to polysubstituted alpha-hydroxytropolones. Organic letters. 2012; 14:5988–5991. [PubMed: 23167954]

Mecozzi S, West AP Jr, Dougherty DA. Cation-pi interactions in aromatics of biological and medicinal interest: electrostatic potential surfaces as a useful qualitative guide. Proceedings of the National Academy of Sciences of the United States of America. 1996; 93:10566–10571. [PubMed: 8855218]

Miyamoto D, Endo N, Oku N, Arima Y, Suzuki T, Suzuki Y. Beta-thujaplicin zinc chelate induces apoptosis in mouse high metastatic melanoma B16BL6 cells. Biological & pharmaceutical bulletin. 1998a; 21:1258–1262. [PubMed: 9881634]

Miyamoto D, Kusagaya Y, Endo N, Sometani A, Takeo S, Suzuki T, Arima Y, Nakajima K, Suzuki Y. Thujaplicin-copper chelates inhibit replication of human influenza viruses. Antiviral research. 1998b; 39:89–100. [PubMed: 9806486]

Murelli RP, D'Erasmo MP, Hirsch DR, Meck C, Masaoka T, Wilson JA, Zhang B, Pal RK, Gallicchio E, Beutler JA, Le Grice SF. Synthetic alpha-Hydroxytropolones as Inhibitors of HIV Reverse Transcriptase Ribonuclease H Activity. MedChemComm. 2016; 7:1783–1788. [PubMed: 28093576]

Oblak EZ, Bolstad ES, Ononye SN, Priestley ND, Hadden MK, Wright DL. The furan route to tropolones: probing the antiproliferative effects of beta-thujaplicin analogs. Organic & biomolecular chemistry. 2012; 10:8597–8604. [PubMed: 23032214]

Prueksaritanont T, Subramanian R, Fang X, Ma B, Qiu Y, Lin JH, Pearson PG, Baillie TA. Glucuronidation of statins in animals and humans: a novel mechanism of statin lactonization. Drug metabolism and disposition: the biological fate of chemicals. 2002; 30:505–512. [PubMed: 11950779]

Raies AB, Bajic VB. In silico toxicology: computational methods for the prediction of chemical toxicity. Wiley interdisciplinary reviews. Computational molecular science. 2016; 6:147–172. [PubMed: 27066112]

Rekka E, Chrysselis M, Siskou I, Kourounakis A. Synthesis of new azulene derivatives and study of their effect on lipid peroxidation and lipoxygenase activity. Chemical & pharmaceutical bulletin. 2002; 50:904–907. [PubMed: 12130848]

Ritchie TJ, Macdonald SJ. The impact of aromatic ring count on compound developability--are too many aromatic rings a liability in drug design? Drug discovery today. 2009; 14:1011–1020. [PubMed: 19729075]

Author Manuscript Author Manuscript Author Manuscript Author Manuscript

Sapse AM, Schweitzer BS, Dicker AP, Bertino JR, Frecer V. Ab initio studies of aromatic-aromatic and aromatic-polar interactions in the binding of substrate and inhibitor to dihydrofolate reductase. International journal of peptide and protein research. 1992; 39:18–23. [PubMed: 1299221]

Takeshita H, Mori A, Kusaba T. An Improved Synthesis of 2,7-Dihydroxytropone (3-Hydroxytropolone). Synthesis. 1986; 1986:578–579.

Tavis JE, Cheng X, Hu Y, Totten M, Cao F, Michailidis E, Aurora R, Meyers MJ, Jacobsen EJ, Parniak MA, Sarafianos SG. The hepatitis B virus ribonuclease H is sensitive to inhibitors of the human immunodeficiency virus ribonuclease H and integrase enzymes. PLoS pathogens. 2013; 9:e1003125. [PubMed: 23349632]

Trepo C, Chan HL, Lok A. Hepatitis B virus infection. Lancet. 2014; 384:2053–2063. [PubMed: 24954675]

van De Waterbeemd H, Smith DA, Beaumont K, Walker DK. Property-based design: optimization of drug absorption and pharmacokinetics. Journal of medicinal chemistry. 2001; 44:1313–1333. [PubMed: 11311053]

van der Spoel D, van Buuren AR, Tieleman DP, Berendsen HJ. Molecular dynamics simulations of peptides from BPTI: a closer look at amide-aromatic interactions. Journal of biomolecular NMR. 1996; 8:229–238. [PubMed: 8953214]

Viswanadhan VN, Ghose AK, Revankar GR, Robins RK. Atomic physicochemical parameters for three dimensional structure directed quantitative structure—activity relationships. IV: Additional parameters for hydrophobic and dispersive interactions and their application for an automated superposition of certain naturally occurring nucleoside antibiotics. Journal of chemical information and computer sciences. 1989; 29:163–172.

Williams YD, Meck C, Mohd N, Murelli RP. Triflic acid-mediated rearrangements of 3-methoxy-8-oxabicyclo[3.2.1]octa-3,6-dien-2-ones: synthesis of methoxytropolones and furans. The Journal of organic chemistry. 2013; 78:11707–11713. [PubMed: 24171600]

Xu L, Hui AY, Albanis E, Arthur MJ, O'Byrne SM, Blaner WS, Mukherjee P, Friedman SL, Eng FJ. Human hepatic stellate cell lines, LX-1 and LX-2: new tools for analysis of hepatic fibrosis. Gut. 2005; 54:142–151. [PubMed: 15591520]

Zhao J. Plant troponoids: chemistry, biological activity, and biosynthesis. Current medicinal chemistry. 2007; 14:2597–2621. [PubMed: 17979713]

Author Manuscript Author Manuscript Author Manuscript Author Manuscript

Highlights

- Efficacy of α-hydroxytropolones against HBV is diminished by bulky substitutions on the troponoid ring
- Carbonyl, lactone, or sulfone groups at R^2 on the troponoid ring enhance activity against HBV
- No cell-specific cytotoxicity was found among cells of hepatic, kidney, or stellate-cell origin
- Cytotoxicity of the troponoids correlated with a hydroxyl in the α position on the troponoid ring and overall lipophilicity

Author Manuscript Author Manuscript Author Manuscript Author Manuscript

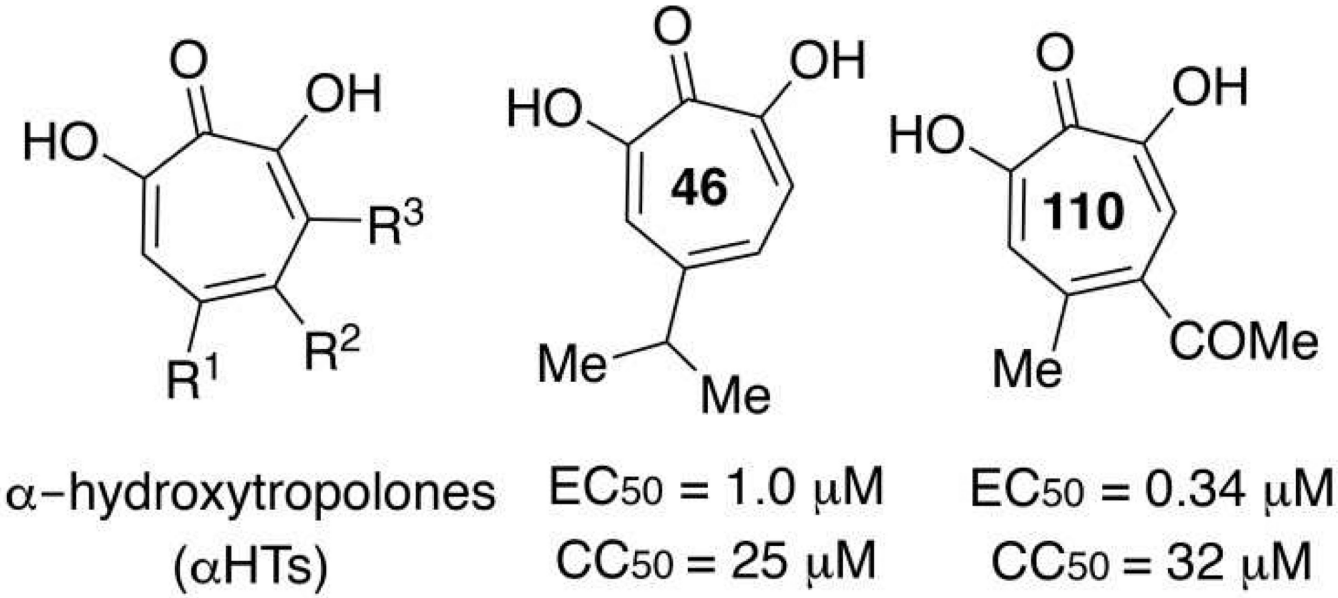

Figure 1.

α-Hydroxytropolone scaffold along with the top antiviral natural product lead b-thujaplicinol (#46) and the top synthetic lead (#110). Data are from (Lu et al., 2015).

Author Manuscript Author Manuscript Author Manuscript Author Manuscript

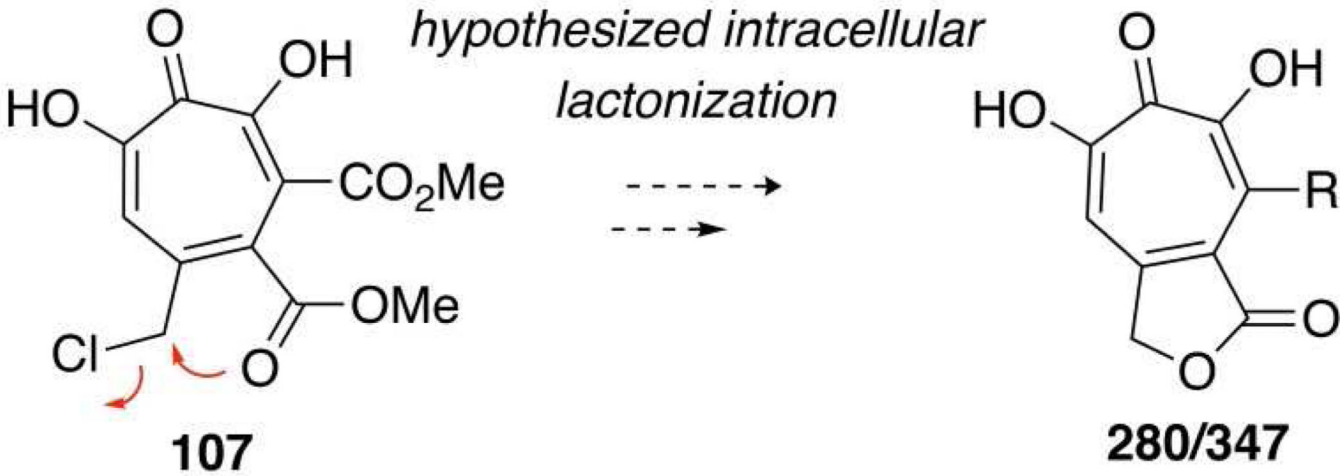

Cmpd	R	EC_{50} (μM)	CC_{50} (μM)	TI
107	-	0.4 ± 0.2	> 80	>200
280	CO_2Me	0.5 ± 0.1	>77	>154
347	H	0.6 ± 0.4	100	167

Figure 2.

Mechanistic overview of proposed cellular lactonization of **#107** to **280**, along with HBV antiviral (EC_{50}) and cytotoxicity (CC_{50}) values of **#107**, and synthesized lactones **#280** and **347**.

Author Manuscript Author Manuscript Author Manuscript Author Manuscript

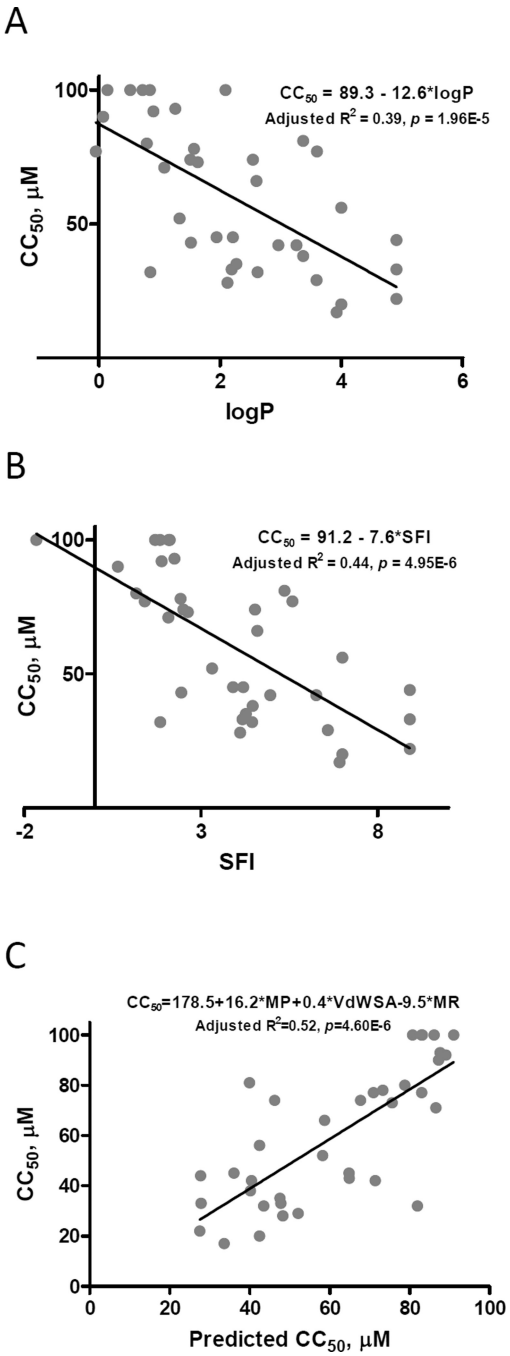

Figure 3.

Correlation of physiochemical properties of the α-hydroxytropolones with cytotoxicity. **A.** logP as predictor of cytotoxicity. **B.** Solubility forecast index (SFI) as predictor of cytotoxicity. **C.** Multivariate linear regression model for cytotoxicity.

Author Manuscript Author Manuscript Author Manuscript Author Manuscript

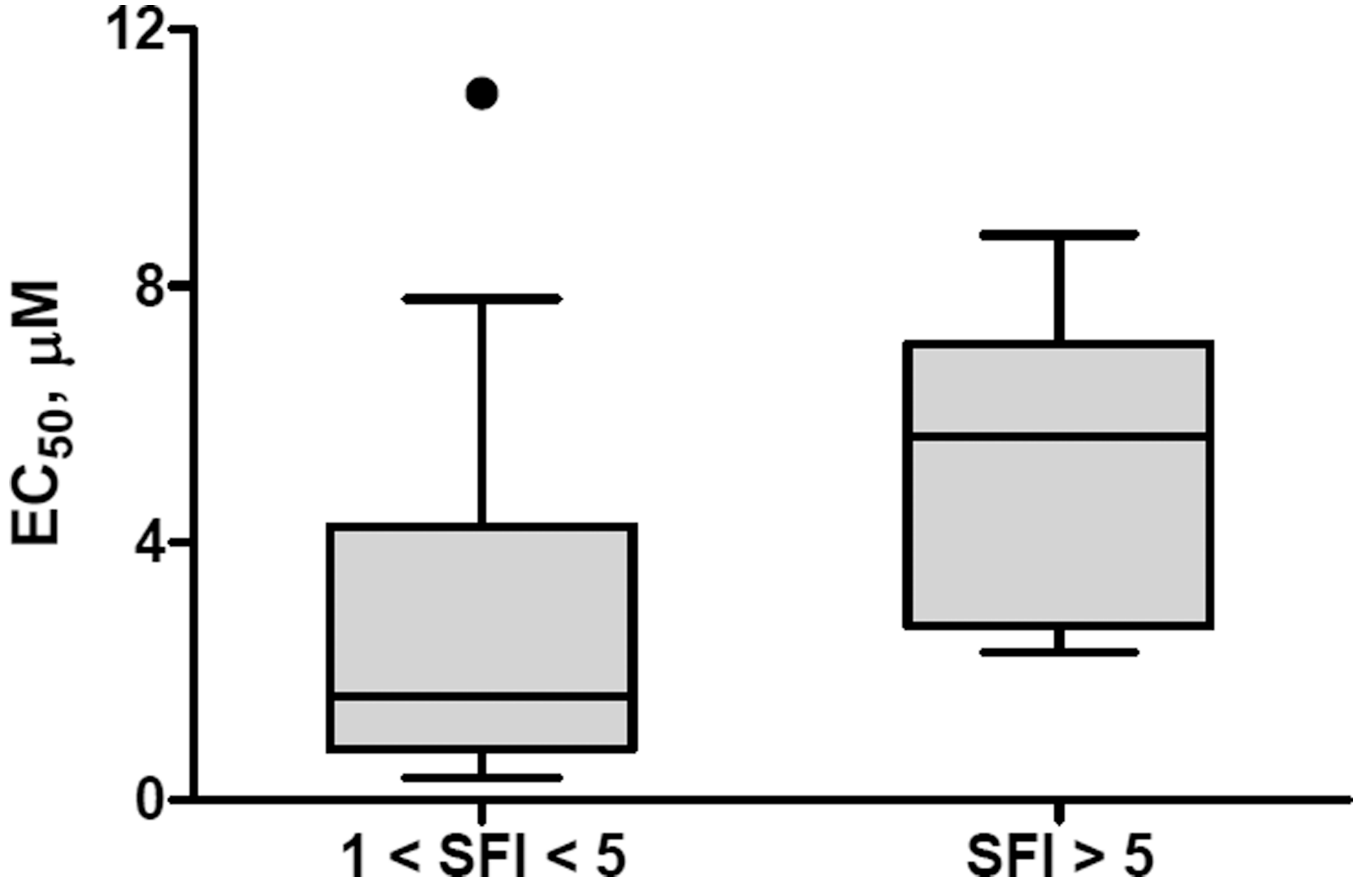

Figure 4.

Lower SFI values correlate with greater efficacy for the α-hydroxytropolones. Box-whisker plots comparing EC_{50}s of α-hydroxytropolones binned by SFI values.

Author Manuscript Author Manuscript Author Manuscript Author Manuscript

Table 1

Activity profile of selected troponoids

Cmpd	R^1	R^2	R^3	EC_{50} (μM)	CC_{50} (μM)	TI
172	H	H	H	1.7 ± 1.3	>100	>59
Mono-substituted αHTs[a]						
46[b]	*i*-Pr	H	H	1.0 ± 0.6	25 ± 20	25
210	CH_3	H	H	1.2 ± 0.8	71 ± 13	59
261	Br	H	H	11 ± 3.5	74 ± 3.3	7
263	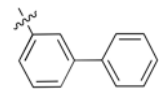	H	H	2.4 ± 0.7	56 ± 7.4	23
264	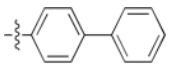	H	H	2.8 ± 0.7	20 ± 9.3	7
Di-substituted αHTs where R^1 = Me and R^2 = Aromatic						
112[b]	CH_3	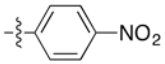	H	2.5 ± 1.3	79 ± 15	32
113[b]	CH_3	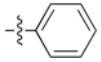	H	4.2 ± 0.8	66 ± 10	16
114	CH_3	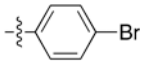	H	4.8 ± 2.4	38 ± 12	8
119	CH_3	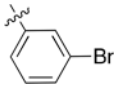	H	6.4 ± 2.6	81 ± 14	13
146	CH_3	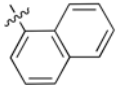	H	2.3 ± 0.6	29 ± 4.3	13
Di-substituted αHTs where R^1 = Me and R^2 = Carbonyl-Containing Appendages and Sulfone #336						

Author Manuscript Author Manuscript Author Manuscript Author Manuscript

Cmpd	R^1	R^2	R^3	EC_{50} (μM)	CC_{50} (μM)	TI
109	CH_3	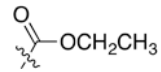	H	4.3 ± 2.0	93 ± 25	22
110[b]	CH_3	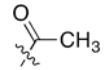	H	0.34 ± 0.03	32 ± 5	94
111	CH_3	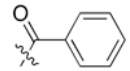	H	0.9 ± 0.7	35 ± 11	39
118	CH_3	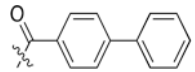	H	6.0 ± 3.2	17 ± 5.0	3
120	CH_3	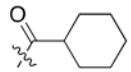	H	3.3 ± 1.6	42 ± 17	13
143	CH_3	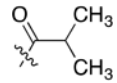	H	4.7 ± 4.4	>100	>21
173	CH_3	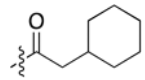	H	6.7 ± 3.8	77 ± 5.8	11
257	CH_3	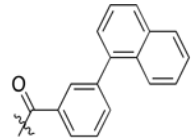	H	8.3 ± 2.4	44 ± 2.8	5
258	CH_3	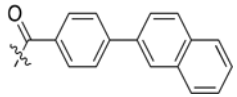	H	8.8 ± 2.4	33 ± 8	4

Author Manuscript Author Manuscript Author Manuscript Author Manuscript

Cmpd	R^1	R^2	R^3	EC_{50} (μM)	CC_{50} (μM)	TI
259	CH_3	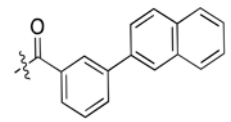	H	2.8 ± 0.9	22 ± 2	8
274	CH_3	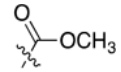	H	1.1 ± 0.8	>92	>84
308	CH_3	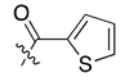	H	1.0 ± 0.5	33 ± 9.5	33
309	CH_3	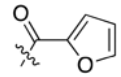	H	1.4 ± 0.8	52 ± 17	37
310	CH_3		H	2.5 ± 0.2	73 ± 20	29
311	CH_3	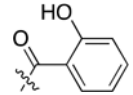	H	1.6 ± 0.8	32 ± 16	20
312	CH_3	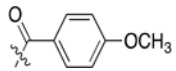	H	0.9 ± 0.6	28 ± 0.8	31
313	CH_3	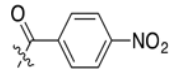	H	0.7 ± 0.7	45 ± 13	64
315	CH_3	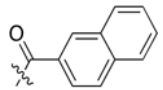	H	5.3 ± 1.1	42 ± 8.7	8
319	CH_3		H	7.2 ± 1.4	>100	>14

Author Manuscript Author Manuscript Author Manuscript Author Manuscript

Cmpd	R^1	R^2	R^3	EC_{50} (μM)	CC_{50} (μM)	TI
336	CH_3	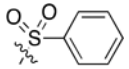	H	0.4 ± 0.2	45 ± 8	130
Tri-substituted α-HTs and Lactones						
106	CH_3	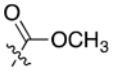	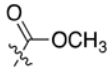	2.7 ± 0.3	38 ± 2	14
107	CH_2Cl	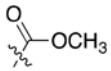	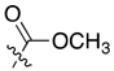	0.4 ± 0.2	>80	>200
108	CH_2OMe	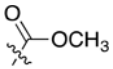	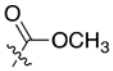	15 ± 2.2	>90	>6
334	CH_3		Br	3.0 ± 1.0	43 ± 4.1	14
335	CH_3	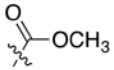	Br	7.8 ± 1.1	78 ± 31	10
280	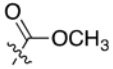		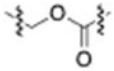	0.5 ± 0.1	>77	>154
347	H		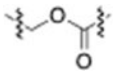	0.6 ± 0.4	100	167

[a] αHT, α-hydroxytropolone

[b] Data from (Lu et al., 2015).

Author Manuscript Author Manuscript Author Manuscript Author Manuscript

Table 2

Cytotoxicity of selected troponoids in three cell lines

Compound	CC_{50}, μM		
	Cell line		
	HepDES19	HEK293	LX2
107	>80	> 100	>100
111	35 ± 11	>83 ± 26	85
172	>100	>100	71
210	71 ± 13	>100	n/a
274	>92	>90	88 ± 7
280	>77	>100	104 ± 31
308	33 ± 9.5	74 ± 49	48 ± 43
309	52 ± 17	86 ± 32	66 ± 27
312	28 ± 0.8	49 ± 31	61 ± 58
313	45 ± 13	44 ± 15	99
347	100	>100	>100